Propagation of a narrow plasma beam in an oblique magnetic field

W. W. Heidbrink, D. Adams, S. Drum, K. Evans, J. Manson, T. Price, P. Urayama, and F. J. Wessel
Department of Physics, University of California, Irvine, California 92717

(Received 30 March 1992; accepted 22 June 1992)

The propagation of an intense neutralized ion beam ($v \sim 5 \times 10^8$ cm/sec, $n \sim 10^{10}$ cm^{-3}) through a large insulated vacuum chamber is measured as a function of magnetic field strength and direction. When the beam propagates parallel to the applied field, beam divergence is reduced. When the beam propagates perpendicular to the applied field, the downstream beam density decreases with increasing field strength. When the beam velocity vector intersects the magnetic field at an oblique angle, beam propagation is determined primarily by the perpendicular component of the field.

The transport of plasma across a magnetic field is a fundamental problem in plasma physics with applications in space physics, astrophysics, strategic defense, and magnetic fusion. In this Brief Communication, we report laboratory measurements of the propagation of an intense, narrow, ion beam. In the study of beam propagation, a distinction is made[1] between large gyroradius, or "narrow" ion beams (in which the ion gyroradius ρ_i is much larger than the beam transverse width y) and "wide" ion beams with $\rho_i/y \ll 1$. Our experiment is conducted in the large gyroradius limit ($\rho_i/y \sim 10$). We employ a "neutralized" ion beam, i.e., a quasineutral plasma with significantly smaller thermal kinetic energy than directed kinetic energy ($T \ll E_i$). The beam is sufficiently intense to form a polarization layer and propagate across a transverse magnetic field via the $\mathbf{E} \times \mathbf{B}$ drift[2] (dielectric constant $\epsilon \sim 3 \times 10^3$). The beam quickly magnetizes when entering the field.[3]

In previous work, the propagation of intense, narrow ion beams was studied in an axial field[4] and in a transverse magnetic field.[2,3,5] Our results extend these studies to the general case of narrow beam propagation at an arbitrary angle with respect to the magnetic field. (Previously, propagation at an oblique angle has been studied only for wide beams.[1]) The beam is formed by a ten-stage Marx generator operated at 225 kV that drives a magnetically insulated ion diode.[6] Flashover of an annular plastic disk that has stainless-steel pins embedded in it creates the hydrogen and carbon beam.[6] The A–K gap is 13 mm, the ratio of insulating field to critical field[6] is $B/B^* \simeq 1.3$, and the pulse duration is ~ 0.5 μsec. The diode gradually degrades over time so all scans are performed sequentially; for these conditions, shot-to-shot variability in the beam intensity is typically 10%. The beam passes through the graphite-coated cathode into an acrylic collimating tube that is 50 cm long and 26 cm in diameter. Measurements with a Rogowski coil placed around the collimating tube indicate that the beam is current neutral to within 1%. After leaving the metallic diode chamber, the beam enters a large fiberglass vacuum chamber (3.0 m long by 1.0 m diameter). Base pressure in the chamber is typically 10^{-5} Torr, so collisions with neutrals have a negligible effect on beam propagation. In the absence of a magnetic field, the beam divergence is $\sim 1\%$. Two independent sets of pulsed magnetic field coils create the magnetic field. The longitudinal (parallel) component of the field is created by solenoidal coils wrapped on the fiberglass chamber. The vertical (perpendicular) component of the field is created by a set of six rectangular windings. The dc fields created by these coils were measured throughout the chamber with a Hall probe and are in excellent agreement with numerical calculations. Agreement with pulsed measurements using a Mirnov coil is also excellent, except near the upstream end of the chamber, where eddy currents in the metallic chamber surrounding the diode partially shield the external field. In the central region of the chamber (> 30 cm from the end flange and $r < 30$ cm), the field is uniform to within 15%.

The diagnostics are similar to those employed by Hong *et al.*[5] Beam intensity is measured with a biased Faraday cup (-550 V) that is inserted vertically into the vacuum chamber through a Wilson seal. (The vertical orientation is employed to minimize the perturbation to the polarization field.) Damage patterns are obtained by exposing sheets of cellulose acetate. A pair of floating potential Langmuir probes that are separated by a known horizontal distance are used to infer the polarization electric field E. Signals from these probes are electronically added with a power splitter/combiner. A probe impedance of 0.8 MΩ gives reproducible results. During beam propagation in a transverse field, the potential difference across the beam can exceed 10 kV. The breakdown strength of the electric field probes was tested by biasing a probe tip to 15 kV while a unmagnetized beam propagated past the probe; no evidence of breakdown was observed.

Propagation is studied both in vacuum and in the presence of a background plasma. The background plasma is created by pulsing current through a row of strip guns coated with titanium hydride. The guns are similar in design to those used previously (Fig. 2 of Ref. 5), but are 1.8 m long. The density ($n \sim 10^{12}$ cm^{-3}) and temperature ($T_e \simeq 10$ eV) of the background plasma is measured with a double-tipped Langmuir probe.

Typical signals for a beam propagating in a transverse field are shown in Fig. 1. Signal begins to appear on a Faraday cup that is approximately 2.1 m from the anode approximately 0.4 μsec after the Marx erects, as expected for protons with ~ 150 keV of energy. A second peak is

 0899-8213/92/103454-03$04.00

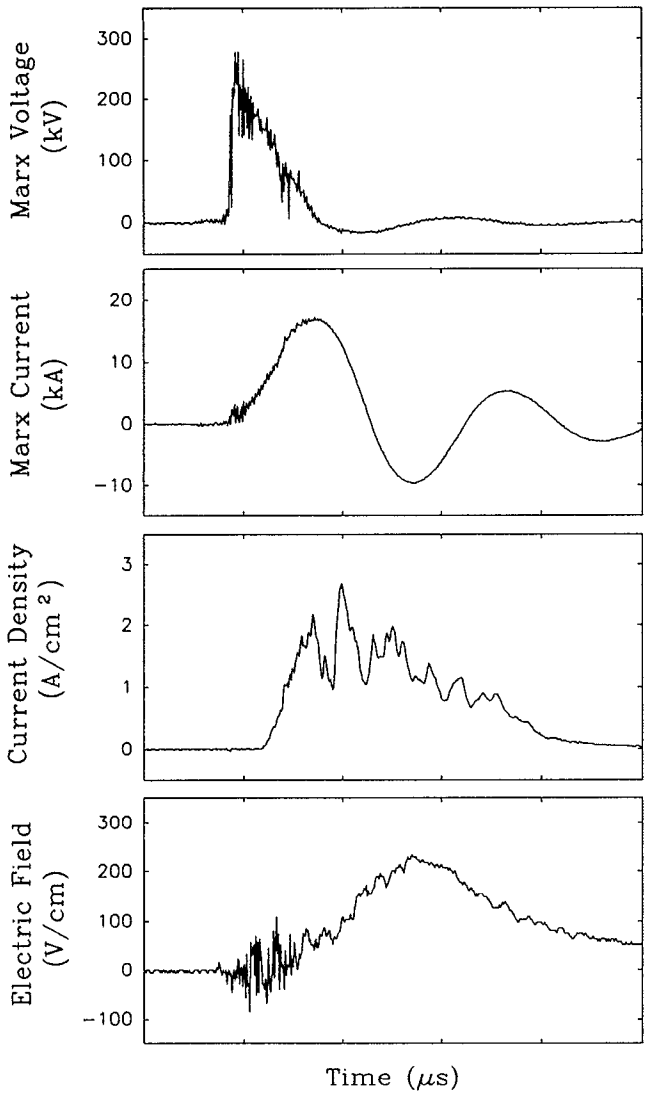

FIG. 1. Typical waveforms for a 225 kV beam injected into a transverse magnetic field (52 G). The Faraday cup (third trace) is located on the symmetry axis 2.1 m from the anode. The Langmuir probes (fourth trace) are separated by 5 cm and are 2.4 m downstream from the anode; the hashy signal when the Marx fires is noise. Note that the Marx voltage falls as the Marx current rises, so beam energies of 100–200 kV are typical.

often observed ~ 1.2 μsec later when carbon ions reach the Faraday cup. In general, the relative amplitudes of the proton and carbon peaks depend on the magnitude and direction of the imposed magnetic field. In our analysis, we digitally average the Faraday signal to obtain a reproducible measure of the beam intensity. The electric field inferred from the floating Langmuir probes is also shown in Fig. 1. For this pulse, the signal is largest when the carbon ions reach the detector location but, for other conditions, the peak electric field occurs earlier, coincident with the proton peak on the Faraday cup signal. In our analysis, we have used the peak value of the electric field signal.

Vertical profiles of the beam are obtained by moving a Faraday cup shot-to-shot (Fig. 2). In the absence of a magnetic field, the beam 2.1 m from the anode is approx-

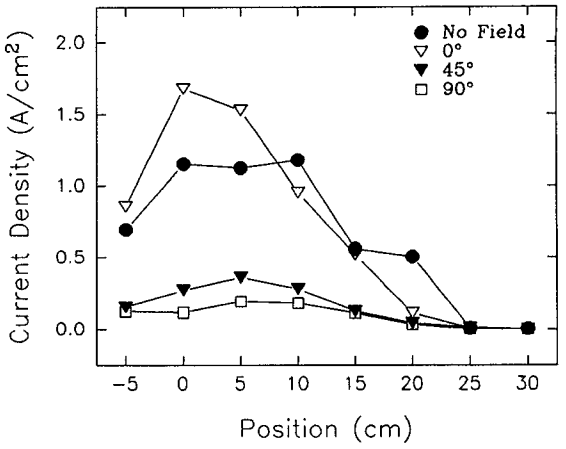

FIG. 2. Peak current density 2.1 m from the anode versus vertical position for four values of B ($B=0$, 250 G). For the cases when $\theta=45°$ and 90°, the peak value occurs when the carbon ions reach the Faraday cup.

imately 0.2 m in height. For an angle between the beam velocity vector and the field of $\theta=0°$, the beam is more intense and the profile is narrower. For $\theta=45°$ and 90°, however, the width of the profile is similar to the $B=0$ case, but the beam intensity is reduced. Damage patterns corroborate the profiles obtained with Faraday cups. In a parallel 250 G field ($\theta=0°$), the damage is relatively intense, approximately circular, and has a ragged margin, as if nonuniformities in the initial beam profile are preserved. In contrast, in an oblique ($\theta=45°$) or perpendicular ($\theta=90°$) 250 G field, the damage is weak and elliptical, with the major axis oriented in the direction of the perpendicular field. Vertical streaks are sometimes observed, perhaps indicating filamentation of the ion beam.

As the magnitude of the field increases, the beam intensity decreases for oblique and perpendicular propagation (Fig. 3). In contrast, for an axial field, the current density tends to increase with increasing field up to $B \simeq 150$

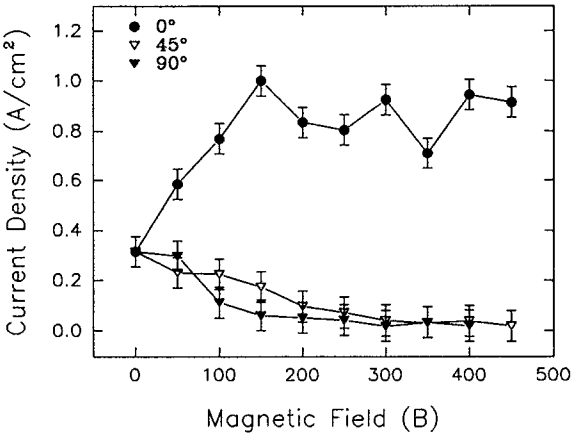

FIG. 3. Current density 2.1 m from the anode versus magnitude of the magnetic field for three different orientations of the field. The current density is averaged for 0.25 μsec at the time of the proton peak. The error bars represent the standard deviation of several shots.

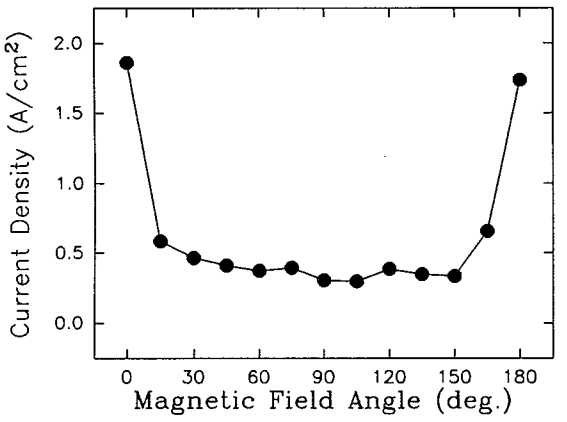

FIG. 4. Current density 2.1 m from the anode versus θ for $B=250$ G. The current density is averaged for 0.25 μsec at the time of the proton peak.

G (Fig. 3). The downstream current density decreases as the propagation angle is varied from $\theta=0°$–$30°$ (Fig. 4). The beneficial effect of an axial field appears to be erased by even a small perpendicular component of the field.

The strength of the polarization electric field depends on the magnitude and direction of **B**. Two regimes are observed: a weak field regime and a strong field regime. The transition between the regimes is seen most clearly by plotting the electric field versus the magnitude of B for $\theta=90°$ (Fig. 5). For $B \lesssim 100$ G, the electric field E increases approximately linearly with B and the magnitude of the field is $E \simeq vB$, where v is the beam velocity. In contrast, for $B \gtrsim 100$ G, the electric field is smaller than vB and the results are irreproducible (Fig. 5). Analysis of the dependence of the electric field signal on the separation of the Langmuir probe tips suggests that beam filamentation may occur in the high field regime. In the low field regime, the voltage across the probes increases approximately linearly with probe separation d, as expected for a uniform polarization electric field. On the other hand, for $B \simeq 250$ G, the signal only increases for $d \lesssim 10$ cm, and becomes

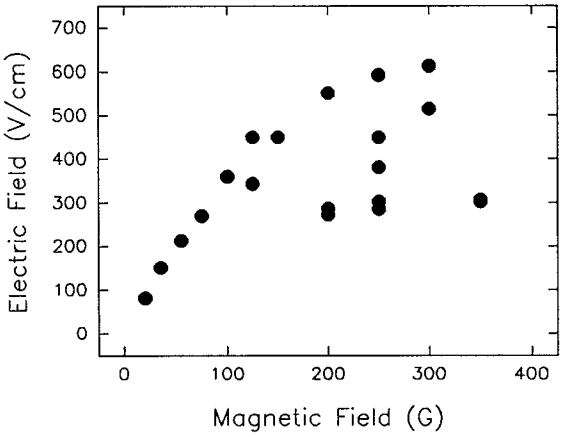

FIG. 5. Electric field signal 2.4 m from the anode versus magnitude of the transverse field ($\theta=90°$). Probe separation $d=10$ cm.

erratic for larger values of d. Similar results are obtained for the dependence of the electric field on magnetic field direction θ. In the low field regime ($B \simeq 50$ G), the electric field increases monotonically as the field is rotated from a parallel to a perpendicular orientation. In contrast, in the high field regime ($B \simeq 250$ G), E tends to increase with θ but the results are irreproducible.

A background plasma causes a reduction in beam intensity for all angles of propagation, but has little effect on the unmagnetized case.

In summary, beam propagation in an oblique field resembles propagation in a transverse field. An electric field transverse to **v** and **B** is established, as for propagation in a transverse field. The signals and parametric dependencies are similar for oblique and transverse propagation, but differ for the axial and unmagnetized cases. The measured beam intensity is consistent with the interpretation that $B_\perp = B \sin\theta$ determines j, independent of the orientation of the field. The perpendicular component of the field $B_\perp$ has the dominant effect on beam propagation.

Propagation in an axial field seems to be a special case. The beam intensity increases with B for $\theta=0°$, but decreases for other angles (Fig. 3). Robertson[4] reported focussing of an intense ion beam in an axial field; for our parameters, a reduction in divergence is observed but the beam is not focused. Only a small amount of perpendicular field nullifies the increase in intensity associated with an axial field (Fig. 4).

There is some evidence for beam filamentation at larger values of B. Previous workers[5] speculated that the deviation in linear scaling of E with B (Fig. 5) was due to shorting to the vessel chamber when the electric field becomes large. In our new chamber, however, the beam is separated by $\gtrsim 20$ cm from the wall, so this explanation seems less plausible.

ACKNOWLEDGMENTS

The assistance of J. Cortese and J. Kiehn is gratefully acknowledged.

This study was supported by U. S. Department of Energy Grant No. DE-FG03-89ER53282, by CalSpace, by the National Aeronautics and Space Administration, and by National Science Foundation Grant No. PHY9100825.

[1] F. J. Wessel, N. Rostoker, A. Fisher, H. U. Rahman, and J. H Song, Phys. Fluids B **2**, 1467 (1990).
[2] S. Robertson, H. Ishizuka, W. Peter, and N. Rostoker, Phys. Rev. Lett. **47**, 508 (1981); Phys. Fluids **25**, 2353 (1982).
[3] F. J. Wessel, R. Hong, J. Song, A. Fisher, N. Rostoker, A. Ron, R. Li, and R. Y. Fan, Phys. Fluids **31**, 3778 (1988).
[4] S. Robertson, Appl. Phys. Lett. **39**, 883 (1981).
[5] R. Hong, F. J. Wessel, J. Song, A. Fisher, and N. Rostoker, J. Appl. Phys. **64**, 73 (1988).
[6] S. Humphries, Jr., *Charged Particle Beams* (Wiley, New York, 1990), Sec. 8.8.